PNNL-26957
RPT-DVZ-AFRI-051

Pacific Northwest
NATIONAL LABORATORY

Proudly Operated by **Battelle** *Since 1965*

Evaluation of Iodine Remediation Technologies in Subsurface Sediments: Interim Status Report

September 2017

CE Strickland
AR Lawter
NP Qafoku
JE Szecsody
MJ Truex
G Wang

U.S. DEPARTMENT OF
ENERGY

Prepared for the U.S. Department of Energy
under Contract DE-AC05-76RL01830

PACIFIC NORTHWEST NATIONAL LABORATORY
operated by
BATTELLE
for the
UNITED STATES DEPARTMENT OF ENERGY
under Contract DE-AC05-76RL01830

Printed in the United States of America

Available to DOE and DOE contractors from
the Office of Scientific and Technical
Information,
P.O. Box 62, Oak Ridge, TN 37831-0062
www.osti.gov
ph: (865) 576-8401
fox: (865) 576-5728
email: reports@osti.gov

Available to the public from the National Technical Information Service
5301 Shawnee Rd., Alexandria, VA 22312
ph: (800) 553-NTIS (6847)
or (703) 605-6000
email: info@ntis.gov
Online ordering: http://www.ntis.gov

Evaluation of Iodine Remediation Technologies in Subsurface Sediments: Interim Status Report

CE Strickland
AR Lawter
NP Qafoku
JE Szecsody
MJ Truex
G Wang

September 2017

Prepared for
the U.S. Department of Energy
under Contract DE-AC05-76RL01830

Pacific Northwest National Laboratory
Richland, Washington 99354

Summary

Isotopes of iodine were generated during plutonium production from nine production reactors at the U.S. Department of Energy Hanford Site. The long half-life ^{129}I generated at the Hanford Site during reactor operations was 1) stored in single-shell and double-shell tanks, 2) discharged to liquid disposal sites (e.g., cribs and trenches), 3) released to the atmosphere during fuel reprocessing operations, or 4) captured by off-gas absorbent devices (silver reactors) at chemical separations plants (PUREX, B-Plant, T-Plant, and REDOX). Releases of ^{129}I to the subsurface have resulted in several large, though dilute, plumes in the groundwater, including the plume in the 200-UP-1 operable unit. There is also ^{129}I remaining in the vadose zone beneath disposal or leak locations. Because ^{129}I is an uncommon contaminant, relevant remediation experience and scientific literature are limited.

Iodine cannot be degraded/transformed to a less toxic form. Therefore, the primary metric for remediation is changing the fate and transport properties in a way that works to decrease radioiodine concentrations in groundwater. To this end, targeted laboratory experiments were conducted to provide proof-of-principle screening of remedial options and to evaluate scale-up and performance elements. The evaluation of different iodine remediation technologies will occur over multiple years and fall into three different categories: 1) geochemical/biological sequestration, 2) microbial volatilization, and 3) enhanced pump-and-treat. This report provides status on two in situ sequestration methods (apatite and iron oxides) and two methods examining enhanced pump-and-treat.

The use of apatite as a method of iodine sequestration is still in progress, but results to date show no iodide uptake and limited (10%) iodate uptake with no sediment present. When iodine-contaminated sediment is present, no measureable iodate or iodide uptake occurs. The initial screening for sequestering iodine in iron oxides has been completed. Results show promise in the ability to sequester iodate, but more mechanistic information is needed to advance the potential technology, such as the influence of particle size on sequestration and the potential for field-scale application. In addition, early results indicate that iron oxides may play an important role in the sequestration of iodate in calcite.

Sodium dithionate experiments are currently in progress to identify its ability to enhance iodine mobility in the subsurface. This may be a viable treatment option given that hydraulic controls are limiting downgradient movement of the iodine plume. The use of strong reductant like sodium dithionate can reduce iodine to iodide, and thereby increase its mobility and likelihood of being treated by the pump-and-treat system. Iodine mobilization can also be enhanced by using a high pH carbonate solution to promote the release of iodate from carbonates. Both technology evaluations have been initiated and will continue into the next fiscal year.

The studies in this report provide valuable information required to evaluate potential remedial technologies for iodine and recommend that additional evaluation efforts continue. This evaluation of potential remediation technology supports the efforts outlined in the *UP-1 Evaluation Plan for Iodine.*[1] These studies are graded as “Basic Research” (see Section 4.0) and the presented graphs and data in this Interim Status report are “For Information Only.”

---

[1] DOE. 2015. *UP-1 Evaluation Plan for Iodine*. DOE/RL-2015-69, Draft A, U.S. Department of Energy, Richland Operations Office, Richland, WA.

Acknowledgements

This document was prepared by the Deep Vadose Zone − Applied Field Research Initiative at Pacific Northwest National Laboratory. Field activities were coordinated by the CHPRC. Funding for this work was provided by the U.S. Department of Energy (DOE) Richland Operations Office. The Pacific Northwest National Laboratory is operated by Battelle Memorial Institute for the DOE under Contract DE-AC05-76RL01830.

Acronyms and Abbreviations

AGW	artificial Hanford groundwater
BET	Brunauer-Emmett-Teller
CAWSRP	Conducting Analytical Work in Support of Regulatory Programs
DDI	distilled deionized
ESL	Environmental Sciences Laboratory
FIO	For Information Only
FY	fiscal year
HASQARD	Hanford Analytical Services Quality Assurance Requirements Document
HFO	2-line ferrihydrite
ICP-MS	inductively coupled plasma mass spectrometry
OU	operable unit
QA	quality assurance
SEM	scanning electron microscope
XRD	X-ray diffraction
ZPC	zero-points of charge

Contents

Figures

Tables

1.0 Introduction

Releases of ^{129}I to the subsurface have resulted in several large, though dilute, plumes in the groundwater at the Hanford Site, including the plume in the 200-UP-1 operable unit (OU). There is also ^{129}I remaining in the vadose zone beneath disposal or leak locations. Because ^{129}I is an uncommon contaminant, relevant remediation experience and scientific literature are limited. Based on samples of 200 West Area groundwater (including samples within the 200-UP-1 OU), iodine is present in the plume as a mix of iodide (I^-), iodate (IO_3^-), and Organo-I species (Figure 1). Plume behavior is affected by differential transport of iodine species due to their different sorption and redox characteristics.

The objective of this study is to evaluate remediation technologies for ^{129}I contamination in the Hanford 200 Area aquifer by quantifying how they affect the fate and transport of iodine species. Detailed description of the ^{129}I plume and factors important for remediation technologies are provided by Strickland et al. 2017 and Truex et al. 2016. Iodine cannot be degraded/ transformed to a less toxic form; therefore, the primary metric for remediation is changing the fate and transport properties in a way that works to decrease the groundwater ^{129}I concentration over time.

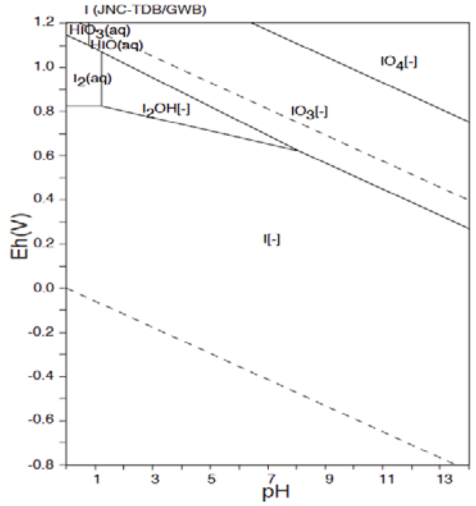

Figure 1. Aqueous iodine stability under different pH and redox conditions.

The evaluation of different approaches to sequester iodine in groundwater will occur over multiple years and include a) geochemical/biological sequestration technologies, b) microbial volatilization technologies, and c) enhanced pump-and-treat technologies. In fiscal year (FY) 2017, two in situ sequestration methods (apatite and iron oxides) and two methods examining enhanced pump-and-treat were evaluated.

1.1 Geochemical and Biological Sequestration of Iodine

The specific geochemical/biological sequestration technologies that will be investigated are as follows:

- In situ precipitation of apatite with iodate incorporation (Campayo et al. 2011)
- Incorporation of iodate and iodide into microbial biomass (i.e., bioaccumulation; Soderlund et al. 2011; Muramatsu et al. 1990a,b; Li et al. 2011)
- Iron oxide/mineral (hematite [Couture and Seitz 1983], pyrite, magnetite, biotite [Fuhrmann et al. 1998]) sorption of iodide/iodate

The apatite sequestration of iodine will include experiments in which artificial groundwater containing iodate or iodide is added to a) apatite precipitates or b) apatite-forming solutions. Microbial bioaccumulation will include experiments in FY18 in which an enriched microcosm of 200-UP-1 sediment will be grown to a high cell density (10^9 cells/mL) and added to artificial groundwater spiked with iodate or iodide. Iron mineral sequestration of iodine will include experiments in which artificial groundwater containing iodate or iodide is added to a) iron minerals and b) iron mineral forming solutions.

For each type of treatment, changes in aqueous-phase iodate/iodide concentration will be monitored and post-treatment presence of iodine in solid phase confirmed. That is, the iodide and iodate uptake in these batch experiments will be characterized by measurement of species uptake (i.e., concentration decrease) from aqueous solution, measurement of iodine mass in solid/surface phases by sequential liquid extractions, and/or identification of precipitates formed by x-ray diffraction (XRD) and iodine uptake by electron microprobe (or other surface-probing techniques).

Laboratory results will be compiled and evaluated in conjunction with consideration of a) long-term iodine species mobility performance (i.e., solubility of a precipitate phase or immobilization of an organic- or microbial-bound iodine); b) ability to emplace the technology at large-field-scale (i.e., advection aspects of the technology in the vadose zone or groundwater); and c) other potential issues associated with field-scale implementation (i.e., potential of technology to mobilize other contaminants, down-gradient effects).

1.2 Enhanced Iodine Mobility for Targeted Pump-and-Treat Application

Enhanced pump-and-treat is an extension of the standard pump-and-treat approach, whereby remedial amendments are added to reinjection waters or otherwise directly injected into a groundwater plume to increase mobility of target contaminants and subsequently increase contaminant mass removal. If contaminant mobility can be increased and the groundwater extraction system is configured to capture the mobilized contaminant mass, then the pump-and-treat efficiency and overall effectiveness can be enhanced. This approach would be potentially applied to enhance pump-and-treat for select “hot-spot”/high concentration portions of the plumes.

Although iodine is generally considered a relatively mobile radionuclide, predominantly as aqueous iodate with a smaller fraction aqueous iodide, previous studies have shown that a significant fraction of the iodine mass can be strongly bound to sediments. Xu et al. (2015) performed sequential extractions on Hanford sediment samples and showed that substantial fractions of sediment-associated iodine was more strongly bound than expected, with the majority associated with calcite incorporation, and to a greater extent, sediment organic carbon. Enhanced mobility of aqueous species as well as these more strongly bound fractions would be the target of an enhanced pump-and-treat system. Recent laboratory experiments (Xu et al. 2015; Truex et al. 2016) have shown that iodate sorption is ~4 times greater than iodide sorption.

Enhanced mobility approaches that will be tested include the following:

- Use of a low concentration of an aqueous reductant (such as sodium dithionate) to reduce iodate to iodide.
- Extraction of iodate from carbonates using a high pH carbonate solution to promote carbonate exchange (and release of iodate from carbonates). This evaluation will be carried out in FY18.

For the reduction of iodate to iodide, low-concentration sodium dithionite will be added to treatments with artificial groundwater containing iodate and 200-DV-1 sediment (high sediment/water ratio). Based on results of batch tests, a column test will be conducted with 200-DV-1 sediments to assess the effluent profile of iodine species for an artificial groundwater influent relative to an influent of artificial groundwater and a low concentration of sodium dithionite. For the release of iodate from carbonates, a solution based on the 1000-hour carbonate extraction media (Kohler et al. 2004) will be added to treatments with artificial groundwater containing 200-DV-1 sediment known to contain iodate-carbonate precipitates (high sediment/water ratio). Based on results of batch tests, a second column test will be conducted with 200-DV-1 sediments to assess the effluent profile of iodine species for an artificial groundwater influent relative to an influent of artificial groundwater amended with a solution based on the 1000-hour carbonate extraction media (Kohler et al. 2004).

For the reduction case, transformation of iodate to iodide based on the aqueous-phase concentration changes will be monitored. For the carbonate exchange case, increases in aqueous-phase iodate concentration will be monitored. In both cases, post-treatment measurement of solid/surface iodine phases will be measured by sequential liquid extraction and/or identification of surface phases by electron microprobe (or other surface-probing techniques).

2.0 Methods

This section describes the experimental methods and is organized by the type of experiment: sequestration and enhanced pump-and-treat. For both categories of experiments, sediments from borehole C9407 were used. Borehole C9407 is located within the vadose zone beneath the T Tank Farm, and has been biogeochemically characterized (Truex et al. 2017). Sediments were used from the 104.4- to 105.4-foot depths (T19 16C, B35443).

2.1 Geochemical Sequestration

2.2 Iodine Sequestration by Apatite Experiments

Iodine and iodate apatite sequestration experiments consist initially of a series of 1-D stop-flow columns in which iodine or iodate is reacted with solid apatite or apatite-forming solutions in contact with sediments at a high sediment/water ratio. Sampling times during these experiments were 2, 21, 93, 165, 215, 385, 765, and 1436 h. The specific experiments are as follows.

- **Control experiment.** A 100-cm by 1.7-cm-diameter column is packed with C9407 sediment (containing field iodine contamination) and no treatment, then aqueous iodine species are measured at times ranging from 0.1 to 1500 hours (experiment D17).

- **Apatite-forming solution and in situ iodide/iodate in sediment.** A 100-cm by 1.7-cm-diameter column is packed with C9407 sediment (containing field iodine contamination) mixed with an aqueous solution of 30 mM phosphate, 40 mM calcium, and 100 mM citrate in river water, then aqueous iodine species are measured at times ranging from 0.1 to 1500 hours (experiment D22). The apatite solution is expected to precipitate about 1.0 g of apatite.

- **Apatite-forming solution and iodate (no sediment).** Batch experiment with 24 mM phosphate, 40 mM calcium, 100 mM citrate, and 150 ug/L iodate in river water and no sediment; aqueous iodine species are measured at times ranging from 0.1 to 1500 hours (experiment D20). The apatite solution is expected to precipitate about 1.0 g of apatite. At the end of the experiment, the ion exchangeable iodine and iodate in phosphate precipitate are measured with a 0.5 mol/L Mg-nitrate solution, then a 0.5 mol/L HNO_3 solution.

- **Apatite-forming solution and iodide (no sediment).** Batch experiment with 24 mM phosphate, 40 mM calcium, 100 mM citrate, and 150 ug/L iodide in river water and no sediment; aqueous iodine species are measured at times ranging from 0.1 to 1500 hours (experiment D21). The apatite solution is expected to precipitate about 1.0 g of apatite. At the end of the experiment, the ion exchangeable iodine and iodate in phosphate precipitate are measured with a 0.5 mol/L Mg-nitrate solution, then a 0.5 mol/L HNO_3 solution.

- **Solid apatite and in situ iodide/iodate in sediment.** A 100-cm by 1.7-cm-diameter column is packed with C9407 sediment (containing field iodine contamination) mixed with 1.0 g of bio-precipitated apatite (see next), then aqueous iodine species are measured at times ranging from 0.1 to 1500 hours (experiment D25). The bio-precipitated apatite consists of 2.0 L of 24 mM Na-phosphate, 40 mM calcium chloride, and 100 mM trisodium citrate at pH 7.5 that was allowed to react in river water for 2 weeks. The precipitate was then washed with groundwater on a 0.22-μm filter and allowed to air dry at room temperature. A higher temperature was not used for drying, as Ca-phosphate precipitates are initially semi-crystalline (which incorporate other metals more rapidly), then more crystalline apatite, which forms after months.

- **Apatite and iodate (no sediment).** Batch experiment with 1.0 g of bio-precipitated apatite in 50 mL of artificial groundwater with 150 μg/L iodate and no sediment (experiment D24). Aqueous iodine species are measured at times ranging from 0.1 to 1500 hours. At the end of the experiment, the ion exchangeable iodine and iodate in phosphate precipitate are measured with a 0.5 mol/L Mg-nitrate solution, then a 0.5 mol/L HNO_3 solution.
- **Apatite and iodide (no sediment).** Batch experiment with 1.0 g of bio-precipitated apatite in 50 mL of artificial groundwater with 150 μg/L iodide and no sediment (experiment D23). Aqueous iodine species are measured at times ranging from 0.1 to 1500 hours. At the end of the experiment, the ion exchangeable iodine and iodate in phosphate precipitate are measured with a 0.5 mol/L Mg-nitrate solution, then a 0.5 mol/L HNO_3 solution.

2.3 Iodine Sorption by Iron Oxides

Iron oxides play an important role in sorption of anionic species in natural environments due to their high zero-points of charge (ZPC). Previous studies (Ticknor and Cho 1990; Yu et al. 1996; Dai et al. 2004, 2009; Nagata et al. 2009, 2010) have shown that iodine can be removed from groundwater through adsorption on iron oxides. For this set of experiments investigating iodine sequestration technologies, iodine immobilization is quantified through sorption or co-precipitation with different iron oxide minerals. In addition, sorption dependence on pH, ionic strength, and iodine concentrations is also identified.

2.3.1 Iron Oxides and Iodine Solutions Preparation

Four iron oxide (and oxyhydroxides) minerals—2-line ferrihydrite (HFO) [$(Fe^{3+})_2O_3 \cdot 0.5H_2O$], magnetite [$Fe^{2+}Fe^{3+}{}_2O_4$], hematite [$\alpha\text{-}Fe^{3+}{}_2O_3$], and goethite [($\alpha\text{-}Fe^{3+}OOH$]—were selected to cover a wide range of iron oxide minerals in the local vadose zone sediments. Because there is no commercially available HFO, the HFO was synthesized in the laboratory using ferric nitrate [$Fe(NO_3)_3 \cdot 9\ H_2O$] as the iron source. The HFO was synthesized using a modified procedure of Schwertmann and Cornell (1991). Briefly, ferric nitrate [8.0089 g of $Fe(NO_3)_3 \cdot 9\ H_2O$] was dissolved into 100 mL distilled deionized (DDI) water in a polyethylene bottle, followed by ca. 65 mL 1 M NaOH dropwise addition while stirring the slurry, until a pH of 13 was achieved. The precipitated HFO was washed using ca. 100 mL DDI water for five times with the help of centrifugation. The final HFO slurry was filtered out using a 0.45-μm vacuum filter and air-dried at room temperature. The air-dried bulk solid HFO was ground to powder using a mortar and pestle, and was confirmed by XRD analysis. The specific surface area of each iron oxide was determined using the Brunauer-Emmett-Teller (BET) method with N_2.

Sodium iodate (>99%) and sodium iodide (>99%) were dissolved into an artificial Hanford groundwater (AGW) to make the IO_3^- and I^-solutions for the sorption and co-precipitation experiments. Based on the reported aqueous iodine concentrations in the Hanford 200 Area iodine plumes (10 pCi [0.57 ppb]) (Truex et al. 2016), iodine spiking solutions were prepared over a range of ca. 4-180 ppb for both iodate and iodide species. Higher concentration solutions were used to account for “hot spots” in the field. In addition, one iodate (35.6 ppb) spiking solution and one iodide (45.7 ppb) spiking solution were prepared in DDI water to check any solution ionic strength impacts on sorption. About 10 L of AGW was synthesized following the recipe from Truex et al. (2017).

Batch sorption experiments for iodate and iodide on the selected four iron oxide minerals were conducted in duplicate using a 50-mL centrifuge tube at room temperature under open air conditions. Based on the results from initial scoping sorption experiments (data not shown), where two solid to solution ratios of 0.4 and 4.0 were tested, solid-to-solution ratios of 2.0 g/L for HFO and 10.0 g/L for magnetite, hematite, and goethite were applied in both iodate and iodide experiments. All the batch reactors were shaken on an orbital shaker at a speed of 70 rpm until the time for sampling. Kinetic uptake experiments for IO_3^- sorption on HFO and goethite, as well as for I^- on HFO and hematite, were performed to determine the reaction times for equilibrium as follows. Briefly, 0.05 g of HFO or 0.25 g of goethite and hematite was put in the centrifuge tubes and filled with 25-mL iodine spiking solutions (36.6 ppb for IO_3^- and 46.2 ppb for I^-). The packed batch reactors were shaken on the orbital shaker for 1, 3, 8, 13, 24, 48, and 241 hours, and the iodate or iodide concentrations at each time interval were monitored. Based on the kinetics, a 48-hour time period was found to be sufficient to establish an apparent sorption equilibrium with the powdered iron minerals used in this study.

The sorption experiments were conducted as functions of pH, ionic strength, and initial iodate or iodide aqueous concentrations. For pH-effect experiments, after the filling of 0.05 to 0.25 g iron oxides and the spiking solutions into the batch tubes, the slurry pH was adjusted using 0.1M NaOH or 0.1M HNO_3 solutions, targeting three final pH values of 5.0, 7.4, and 9.0 to cover the general Hanford Site vadose zone pH conditions. To check any potential solution ionic strength impacts on iodate or iodide sorption on iron oxide minerals, the prepared iodate or iodide spiking solutions in DDI water were applied in a HFO or hematite system under neutral pH (~7.4) conditions.

Finally, a series of iodate or iodide solutions, covering a concentration range of about 4 to 181 ppb, were applied in multiple reaction batch vials in order to test the sorption capacities of iodate or iodide on each tested iron oxide minerals. At the end of the reaction times (48 hours), the batch reactors were centrifuged at 3000 rpm for 20 minutes to separate the sorbent particle from the supernatant. About 3 mL of supernatant solution was sampled from each reactor using pipette, and followed by filtration through a 0.2-µm filter. The filtered solution was delivered to inductively coupled plasma mass spectrometry (ICP-MS) for iodate or iodide concentration measurements. After the 3 mL supernatant sampling, the final supernatant pH was measured using a digital pH meter Accumet Excel- XL15, where the coupled glass pH electrode was calibrated with three buffer solutions (pH 4, 7, and 10) at room temperature. Along each experimental set, duplicated iron oxide-free control vials were also prepared and treated in the same manner that was used for the sorption reactor vials.

The distribution coefficient (K_d) of iodate or iodide for each batch reactor system was determined using a mass balance approach from measurements of the total mass of IO_3^- or I^- added to each batch system and the observed solution concentrations in the aqueous supernatant (C_w) at equilibrium as below:

$$K_d = \frac{C_0V - C_w(V + V_{pH})}{mC_w} \tag{1}$$

where C_0 [µg/L] denotes the measured sorbate concentrations in the iron oxide-free control vials, V denotes the volume of AGW or DDI [L] in each batch reactor vials, V_{pH} denotes the added solution volume [L] of 0.1 M NaOH or 0.1M HNO_3 in each sorption reactor vials for solution pH adjustments, and m [kg] denotes the mass of iron oxides in each batch reactor vial.

The effects of solution IO_3^- or I^- concentrations on each tested iron oxide are described using the sorption isotherms at room temperature. The experimental sorption data conducted at five iodate or iodide concentration levels for each iron oxides was fitted with Freundlich isotherm model:

$$C_s = K_{Fr} C_w{}^{1/n} \tag{2}$$

where C_s [µg/kg] denotes the sorbate concentrations in the solid phase and K_{Fr} [µg/kg : $(\mu g/L)^{1/n}$] and 1/n [-] are the Freundlich coefficients, which measure the sorption capacity and the sorbent's energetic surface heterogeneity, respectively.

2.3.2 Iodine Sequestration during HFO Precipitation (Co-precipitation)

Iodate or iodide sequestration experiments through HFO precipitation in the AGW solution were conducted in duplicate in 125-mL polyethylene bottles. Following the HFO synthesis procedures (Schwertmann and Cornell 1991), the iodine-HFO incorporation experiments were conducted by dissolving 4.0045 g of ferric nitrate [$Fe(NO_3)_3 \cdot 9\ H_2O$] into IO_3^- (34.8 ppb) or I^- (32.9 ppb)-spiked AGW solutions and stirred for 25 minutes on a stir plate. After that, 30 mL 1M NaOH solution (prepared in DDI water) was added into the slurry and stir-mixed for another 40 minutes. After the mixing, the slurry was centrifuged at 2500 rpm for 30 minutes. A volume of 2.5 mL of the centrifuged supernatant was sampled using a pipette and filtered through a 0.2-µm filter for IO_3^- or I^- concentration measurements using ICP-MS. The supernatant pH in the reactors was monitored using the digital pH meter.

To test any kinetic effects of iodine incorporation into the precipitated HFO, an extra 2 mL of supernatant was sampled 20 hours later, and any potential supernatant pH changes were also monitored. To test for any pH effects on the fate of the co-precipitated iodine in the HFO precipitation systems, the pH of the remaining slurry in the co-precipitation reactor was stepwise increased by 1M NaOH (~1 mL for each step) adding to pH 7 and then pH 9. For each step, the slurry was mixed for 40 minutes, centrifuged, and then rested for 20 hours, followed by the supernatant sampling for concentration measurements and pH monitoring. After all procedures were completed, the final solid phase in the reactors were centrifuged and filtered out of solution using a 0.45-µm vacuumed filter. The filtered solid was air-dried for 4 days, followed by solid mass measurements.

2.4 Iodine Mobilization by Na-Dithionite and Carbonate Solutions

Iodine and iodate apatite enhanced pump-and-treat experiments consist initially of a series of 1-D stop-flow columns in which sediment iodine or iodate is reacted with dithionite or carbonate solutions in contact with sediments at a high sediment/water ratio. Sampling times during these experiments were 2, 21, 93, 165, 215, 385, 765, and 1436 hours. The same control (i.e., no treatment, D17) experiment described in Section 3.1 is used. The specific experiments testing mobilization of iodine species are as follows:

- **Sodium dithionite and in situ iodide/iodate in sediment.** A 100-cm by 1.7-cm-diameter column is packed with C9407 sediment (containing field iodine contamination) mixed with an aqueous solution of 60 mM sodium dithionite and 240 mM potassium carbonate (pH 11.5) in anaerobic artificial groundwater water, then packed into the sediment column in an anaerobic chamber (experiment D18). The aqueous iodine species are measured at times ranging from 0.1 to 1500 hours.
- **Carbonate solution and in situ iodide/iodate in sediment.** A 100-cm by 1.7-cm-diameter column is packed with C9407 sediment (containing field iodine contamination) mixed with an aqueous solution of 14.4 mM $NaHCO_3$ and 2.8 mM Na_2CO_3 (pH 9.3) in artificial groundwater water, then packed into the sediment column (experiment D19). The aqueous iodine species are measured at times ranging from 0.1 to 1500 hours.

Because large, increasing iodine concentrations were measured in the dithionite-sediment experiment (D18), it was hypothesized to be caused by 1) actual iodine release from sediment as a result of Fe oxide (or other phase) dissolution; 2) sulfur species interference with the ^{127}I analysis; or 3) iodine in the dithionite or carbonate chemicals. To address these potential causes, additional samples of solutions were analyzed for iodine speciation that included a) 60-mM sodium dithionite and 240-mM potassium carbonate (pH 11.5) solution only [testing hypothesis 3]; b) 60-mM sodium dithionite and 240-mM potassium carbonate (pH 11.5) solution, air sparged for 1 hour to oxidize the dithionite [testing hypothesis 3]; c) 60-mM sodium dithionite and 240-mM potassium carbonate (pH 11.5) solution with 150 ug/L iodate [testing hypothesis 2]; and d) 60-mM sodium dithionite and 240-mM potassium carbonate (pH 11.5) solution with 150 ug/L iodide [testing hypothesis 2].

3.0 Results

This report provides interim results of experiments that are currently ongoing and all discussions, figures, and tables are considered For Information Only (FIO).

3.1 Iodine Sequestration by Apatite

Iodate has recently been reported to incorporate into hydroxyapatite (Campayo et al. 2011). The specific conditions of those experiments included a pH range of 10 to 12 (optimal pH for apatite precipitation is pH 7.5) in deionized water containing only calcium and phosphate. The initial iodate/phosphate ratio was 0.33. The experiments in this study used Hanford-specific geochemical conditions (i.e., Ca, Mg-carbonate saturated artificial groundwater at pH 7.5 in contact with sediments at a high sediment/water ratio) to evaluate whether iodide or iodate incorporates into apatite during precipitation or into solid phase apatite.

3.1.1 Iodide and iodate Uptake During Apatite Precipitation

The two experiments were performed that contained only the apatite solution (and no sediment). Solutions containing 140 μg/L iodide (experiment D21) showed no uptake, and 145 μg/L iodate (experiment D20) showed a small amount of uptake after 384 hours, as measured by the total aqueous ^{127}I (Figure 5). The iodine speciation analysis is in progress. The solution of 24 mM phosphate, 40 mM calcium, and 100 mM citrate (i.e., which forms Ca-citrate complex initially) mixed in river water slowly precipitated apatite over 100 to 200 hours, as shown by the decrease in aqueous phosphate in tens of hours (Figure 2), resulted in 0.5 g of apatite.

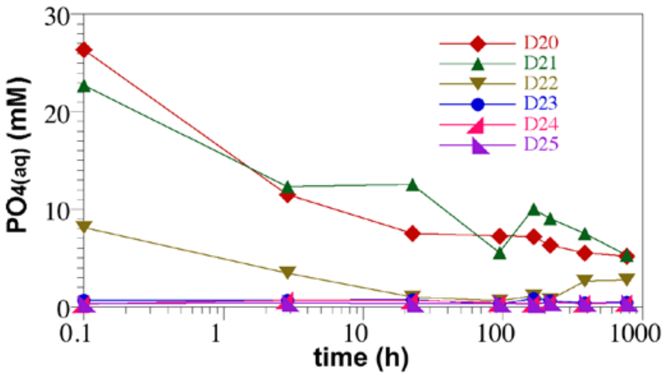

Figure 2. Measurement of aqueous PO_4 showing the time scale of apatite precipitation. Results are FIO.

Measurement of the mass of iodide or iodate sorbed and/or incorporated into apatite shows that both iodide and iodate sorb strongly to apatite (K_d = 4.99 and 5.83 mL/g, respectively, Table 1). There was no measured iodide incorporated into apatite, but 10% of the aqueous iodate was incorporated into apatite. Note that the phosphate/iodate mole fraction was 85,500, using realistic values of phosphate concentration (30 mM) and a realistic maximum aqueous iodate concentration (145 μg/L). The iodate uptake in apatite was very inefficient at these concentrations compared with that reported in a previous study (Campayo et al. 2011) at a phosphate/iodate mole fraction of 3.0 (and without other aqueous ions). Experiments at different phosphate/iodate ratios (and pH) may change the uptake efficiency.

Table 1. Iodide and iodate sorption and incorporation into apatite. Sediment samples used 375 g of material (third column).

#	species	sed. (g)	PO4 source	PO4/I-127 (mol/mol)	sorbed fraction	Kd (mL/g)	incorporated fraction
D20	iodate	none	Ca-citrate-PO4	26300	0.051	5.83	0.078
D21	iodide	none	Ca-citrate-PO4	27200	0.047	4.99	0.000
D22	iodide, iodate	375	Ca-citrate-PO4	20600, 1270*	--	--	--
D23	iodide	none	solid apatite	25600	0.012	1.18	0.000
D24	iodate	none	solid apatite	37400	0.012	1.06	0.001
D25	iodide, iodate	375	solid apatite	20600, 1270*	0.010	1.06	--
D17	iodide, iodate	375	none	--	--	--	--

* of aq+ adsorbed I-127, total I-127 in sediment

3.1.2 Iodide and Iodate Uptake by Solid Apatite

Iodide and iodate reactivity with solid apatite showed a small amount of sorption, but no uptake in apatite over the 770-hour experiments. With an initial concentration of 149 μg/L iodide and phosphate/iodide molar ratio of 25,600, the aqueous iodide concentration decreased slightly (Figure 3a). The analyzed adsorbed iodide indicated 1.6% was adsorbed (K_d = 1.2 mL/g) and no uptake within apatite (Table 1). The aqueous phosphate concentrations were < 0.3 mM (Figure 2), so the apatite remained a precipitate. Iodate (at 141 μg/L) reaction with solid apatite with a phosphate/iodide molar ratio of 37,400 showed no decrease in the aqueous iodide concentration (Figure 3b). The analyzed adsorbed iodide indicated 1.0% was adsorbed (K_d = 1.06 mL/g) and no uptake within apatite (Table 1).

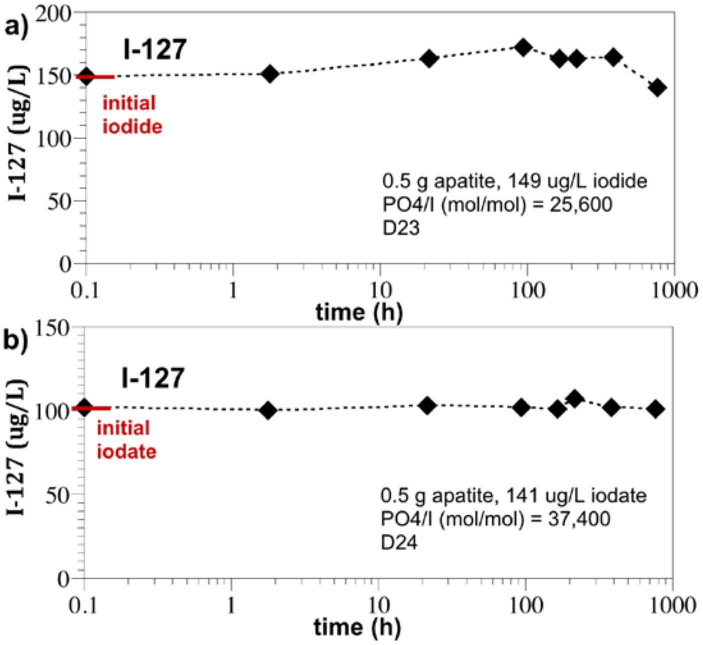

Figure 3. Reaction of solid apatite in batch vials (no sediment) with a) 149 μg/L iodide, and b) 141 μg/L iodate. Results are FIO.

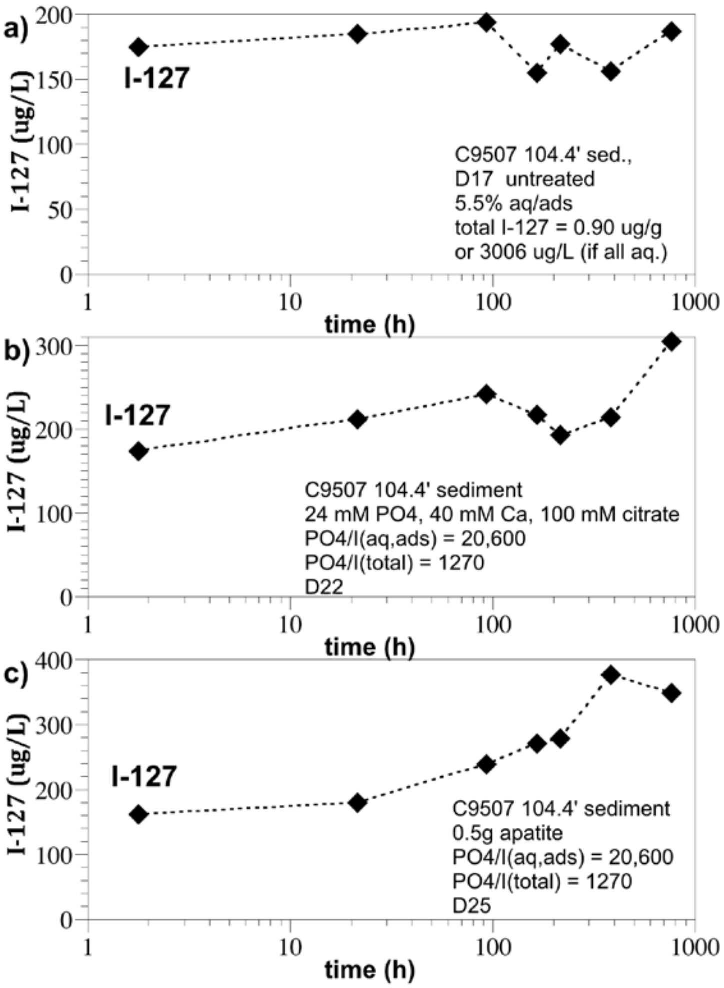

Figure 4. Behavior of iodine-contaminated sediment (C9507, 104.4-105.4') with a) no treatment, b) Ca-citrate-PO_4 solution, and c) solid apatite. Results are FIO.

3.1.3 Apatite Addition to Iodine-Contaminated Sediment

Previous characterization studies with untreated sediments have shown that iodine mass is mainly in solid phases, with 3.9% aqueous, 1.6% adsorbed, 26% in the pH 5 acetate extraction, 38% in the pH 2.3 acetic acid extraction, and 20% in the oxalate extraction (Truex et al. 2017). In Truex et al. 2017, leaching behavior with initial advection of the aqueous and adsorbed fractions was followed by slow release of iodine. This was likely from the dissolution of carbonates or other iodine-bearing phases. The aqueous and adsorbed fraction was 85% iodide.

Reactivity of the Ca-citrate-phosphate solution and solid phase apatite with iodine-contaminated sediment was investigated to evaluate iodine species uptake by apatite. Reaction of the C9507 sediment with artificial groundwater in a stop-flow column in this study showed a relatively constant concentration of ~185 µg/g ^{127}I (Figure 4c). This was equivalent to the aqueous and adsorbed ^{127}I mass calculated from extractions (Truex et al. 2017). Note that if the total ^{127}I in all solid phases were in the pore water, the ^{127}I concentration would be 3006 µg/L. For apatite to be a viable remediation technology, the aqueous and adsorbed ^{127}I would uptake into apatite during initial precipitation, and any additional ^{127}I slowly released from the sediment (from mineral dissolution) would also be uptaken by solid phase apatite.

With a 30-mM phosphate solution in the pore water of a 1-D column filled with the C9507 sediment, about 0.5 g of apatite should precipitate. The apatite to total iodine species ratio (20,600 assuming only aqueous and adsorbed apatite) is lower than in batch experiments showing no iodide uptake (Figure 4a), or limited iodate uptake (Figure 4b).

Results of batch experiments showed that the total aqueous ^{127}I increased from 174 µg/L (at 1.7 hours) to 305 µg/L at 770 hours (Figure 4b). Therefore, not only is there no net iodine uptake from aqueous and adsorbed phases, there is additional dissolution of solid phase(s) resulting in an increase in aqueous ^{127}I. The high ionic strength of the Ca-citrate-phosphate solution and lower carbonate concentration in the solution may have led to dissolution. The sequential extractions (adsorbed and PO$_4$-associated) are in progress, but will likely be inclusive because of the significant additional iodine mass associated with solid phase(s) in the sediment. With the addition of 0.5 g of solid apatite, the total aqueous ^{127}I also increased over time Figure 4c) to 349 µg/L. Therefore, results to date show limited (10%) uptake of iodate and no iodide into apatite with no sediment present, and no measureable iodate or iodide uptake with the same mass of apatite in the presence of iodine-contaminated sediment.

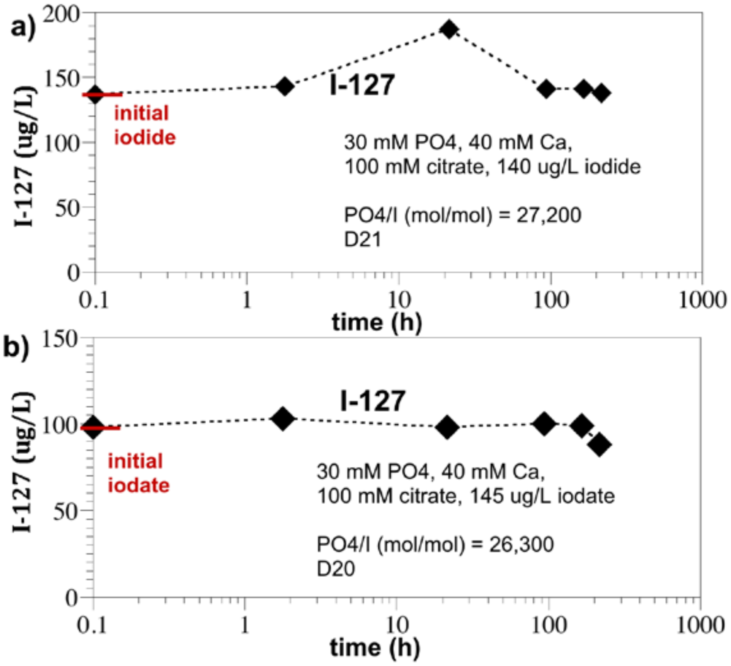

Figure 5. Precipitation of apatite in batch vials from a Ca-citrate-PO$_4$ solution and no sediment with a) 140 µg/L iodide, and b) 145 µg/L iodate. Results are FIO.

3.2 Iodine Sorption by Iron Oxides

3.2.1 Solid Characterization on Iron Oxides

The detailed XRD analysis and scanning electron microscope (SEM) analysis for the four iron oxides tested have been conducted in Chung et al. 2014, and the results are reprinted in Figure 6. For ferrihydrite, its powder XRD pattern contains only two or six scattering bands in its most disordered state. The observed two broad XRD patterns of the synthesized ferrihydrite in the present study were typical for 2-line ferrihydrite (HFO), which agrees with its bulk material morphology in the SEM image. The other three iron oxides showed well-crystalized minerals that matched well with their individual JADE XRD reference peak. The specific surface areas measured by N_2-BET for each iron oxide were 306.90, 6.91, 4.77, and 18.3 m^2/g for HFO, magnetite, hematite, and goethite, respectively. Among the four iron oxides, the relatively low BET specific surface area for magnitude, hematite, and goethite could be supported by their well-crystallized micrometer-sized grain particles (Figure 6). In contrast, the synthesized HFO only existed as a fine-grained and highly defective nanomaterial, which resulted in its higher surface area with micro-pores (0.21 m^3/g with an average pore size of 2.7 nm, based on N_2-BET).

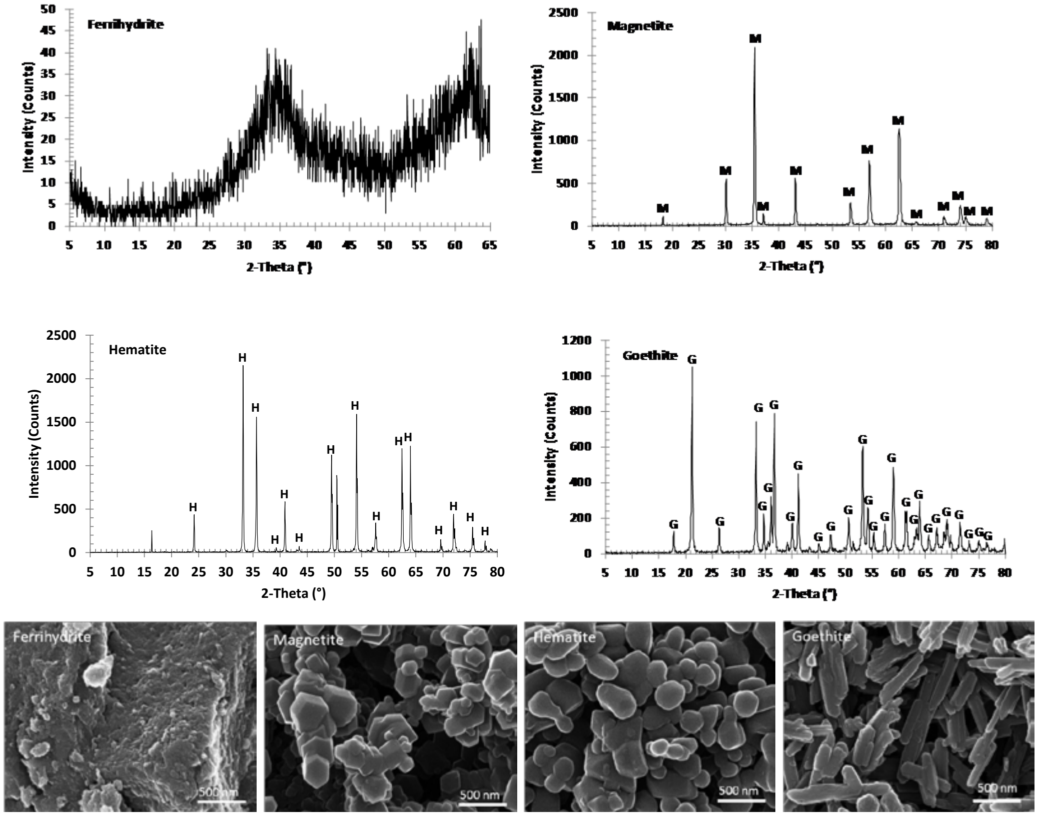

Figure 6. The XRD and SEM analysis showing the typical iron oxide mineral patterns and morphology for each iron oxide tested in the present study (reprinted from Chung et al. 2014). Image scales are approximate.

3.2.2 Sorption Kinetics of Iodine on Iron Oxides

The sorption kinetics of iodate or iodide on HFO, goethite, and hematite in the AGW are presented in Figure 7. For the IO_3 – goethite system, the adsorbed amounts of iodate remained near constant after 8 hours within the examined 241-hour reaction time (Figure 7a). In contrast, for IO_3 – HFO system, the absorbed iodate increased with reaction time (Figure 7a). The slow uptake of iodate in HFO implies that the uptake of IO_3^- could be diffusion-controlled, where the diffusion of IO_3^- into the HFO micro-pore domains likely occurred. This observation is consistent with the N_2-BET results, in which about 0.21 cm^3/g pore volumes with an average pore size of ~2.7 nm was determined. Relative to HFO, the gentle slope for goethite (Figure 7a) implies that the diffusion-controlled IO_3^- transport in the goethite domain might still be occurring, but is still very limited due to its low specific surface area (~18 m^2/g). The low BET surface area implies a smaller possibility for micro-pores to exist.

In the I^-– hematite system, Figure 7b shows that the I^- adsorption on hematite occurred rapidly, where the I^- sorption uptake plateaued after a 1-hour reaction time. This implies that the uptake of iodide by hematite could be mainly through an instant surface adsorption process (assuming equilibrium after 48 hours). This agrees with the N_2–BET results, in which a low specific surface area of ~4 m^2/g was determined for hematite.

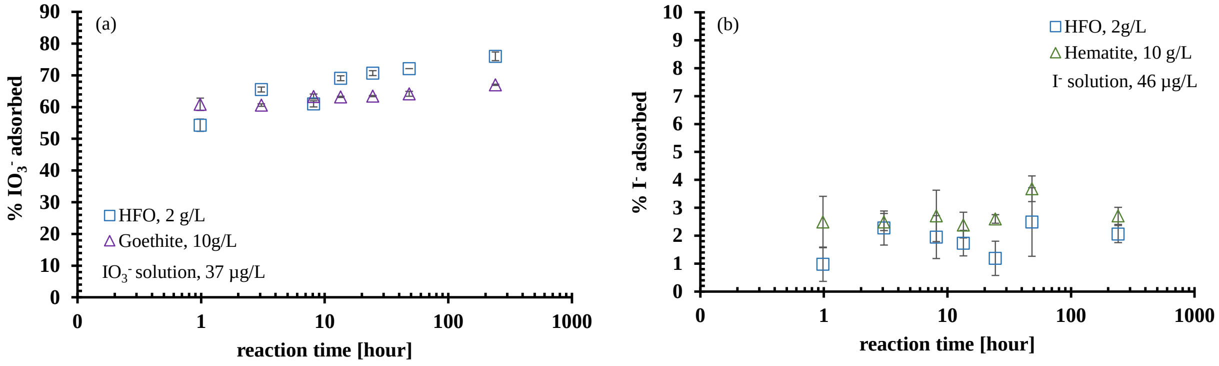

Figure 7. Sorption kinetics of a) iodate on HFO and goethite, and b) iodide on HFO and hematite in the AGW at room temperature.

Iodate sorption for the four iron oxides under different iodate concentrations at neutral pH (pH ~7.3) are plotted in Figure 8. The data were fitted to a Freundlich isotherm model in both nonlinear (Figure 8a) and linear (Figure 8b) plots, and its parameters are listed in Table 2. The model fittings were confident with the R^2 values of 0.96 to 0.99. The determined $1/n$ values (indicating sorbent's energetic surface heterogeneity) among all the tested iron oxides are close to 1 (0.89 to 1.19), indicating near-linear sorption on these pure sorbent materials. This means that the adsorption extent of IO_3^- on the tested iron oxides was not concentration dependent.

These results are consistent with a study of sediments from the Savannah River Site, where the concentration of IO_3^- and I^- in solutions was shown to be significantly affected by the mobility of iodine (Emerson et al. 2014). Among the tested samples, the determined sorption capacity (K_{Fr}) was on the order of HFO > goethite > magnetite > hematite, similar to the results presented in Figure 7a and Table 2. The same sequence was found in terms of the determined N_2-BET specific surface area as 306.90 > 18.3 > 6.91 > 4.77 m^2/g, indicating that surface area controlled iodate adsorption. In this study, HFO showed a far higher sorption affinity for IO_3^- (K_{Fr} of 1279) than other iron minerals due to its large surface area (several hundred square meters per gram). In addition, HFO generally has a high density of local or point defects such as dangling bonds and vacancies. These properties also confer a high absorbing capacity, providing a strong and extensive interaction with many geochemical species.

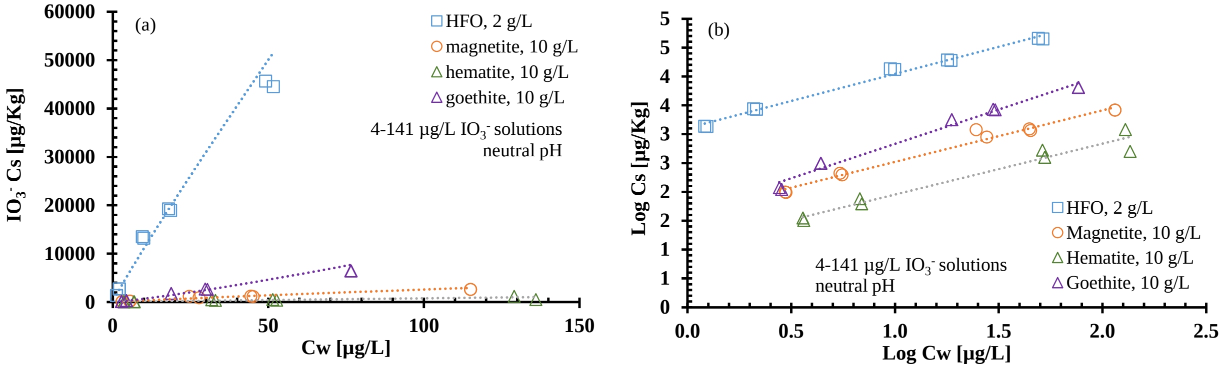

Figure 8. a) Non-linear and b) linear fitting plots of Freundlich isotherm model for the sorption of iodate on the four iron oxide minerals investigated.

Table 2. Freundlich isotherm parameters for iodate (IO_3^-) sorption on HFO, magnetite, hematite, and goethite.

Model parameters	2-line Ferrihydrite	Magnetite	Hematite	Goethite
K_F	1279	42	12	44
1/n	0.94	0.89	0.92	1.19
R^2	0.99	0.98	0.96	0.98

The sorption of iodide on the iron oxides within the concentration range of ca. 4-181 ppb at neutral pH (pH ~7.3) is plotted in Figure 9, where nearly no significant sorption is observed. Similar results were also reported in previous studies. For example, Whitehead (1974) found that freshly precipitated HFO adsorbed substantial amounts of iodide from solutions of pH < 5.5, but the amount decreased to zero as the pH approached 7. Ticknor and Cho (1990) tested adsorption of iodide to hematite and goethite in diluted synthetic groundwater with a pH of ~7.5, and reported that iodide adsorption may have been limited due to the pH and ionic strength of the background solution, similar to the results of this study.

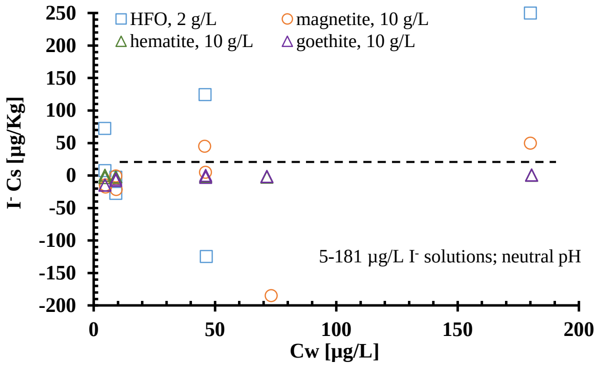

Figure 9. Sorption of iodide on the tested four iron oxides covering a solution concentration range of ca. 4-180 ppb.

3.2.3 Impacts of pH and Ionic Strength on Iodine Sorption on Iron Oxides

The sorption of iodate on HFO, magnetite, hematite, and goethite in AGW solution as a function of pH or ionic strength is illustrated in Figure 10a. Within the tested experimental conditions, the amount of iodate sorption increased concomitantly with the decreasing pH among all the tested iron oxide samples. For example, the K_d values on HFO decreased from 5025 to 569 mL/g with the pH increases from 6.1 to 7.9 (Figure 10a). This is consistent with the general surface acid-base properties of the iron oxides, where an increase in surface charge from negative, through the ZPC, to positive values are presented with the decrease of the solution pH. The adsorption of anions such as IO_3^- is favored only when the pH is lower than the ZPC values; thus, the adsorbent surface is positively charged.

In the present study, within the tested pH range of 4.5 to 8.1, adsorption of IO_3^- was observed on all samples. This could indicate that ZPC values of greater than 8.1 can be assumed for all the tested iron oxide minerals in the synthesized AGW solutions. Calculated K_d values varied from 9 to 5025 mL/g, depending on both the AGW solution pH and the different iron oxide materials. Despite the IO_3^- sorption dependence on pH, within the tested pH ranges, the HFO showed the highest sorption capacity in the AGW solutions. For example, compared to iodate sorption on other iron oxides at low pH (4.5 to 6.5), where the highest sorption capacity presented for each iron oxide minerals (42 to 310 mL/g for magnetite, hematite, and goethite), the HFO still showed much higher sorption capacity (569 mL/g), even at its highest pH condition (pH ~7.9). These results indicate that HFO could be a very promising sorbent for IO_3^- immobilization.

The influence of ionic strength on iodate sorption was observed by comparing IO_3^- sorption on HFO or hematite between the synthesized AGW and DDI water systems. Compared to AGW system, the DDI water system served as a low ionic strength solution system. Figure 10a shows that much higher iodate sorption capacities (K_d) on both HFO and hematite were observed in the DDI water system than in the AGW system. For example, a K_d value of 6874 mL/g for HFO was determined in the DDI water system at a pH of 7.2, which is much higher than the value of 5015 mL/g in the AGW system at an even lower pH condition of pH 6.1. For hematite, with a similar solution pH condition (pH of 6.3 to 6.5), the iodate sorption K_d on hematite is one order of magnitude higher in the DDI water system (739 mL/g) than in the AGW system (42 mL/g). Although the influence of the ionic strength of the aqueous phase on iodine sorption has not been well documented in the literature, these results indicate that the ionic strength has a negative impact on iodate adsorption on iron oxides at near-neutral pH conditions.

The iodide sorption for the four iron oxides in the AGW solution at different pH conditions (pH = 4.5 to 8.3) is illustrated in Figure 10b. Results do not reproduce well in the duplicated reaction vials because of near zero sorption observed for all test conditions. Although a very limited amount of iodide sorption was observed on HFO and hematite, no significant iodide sorption for the four iron oxide samples can be reported to date.

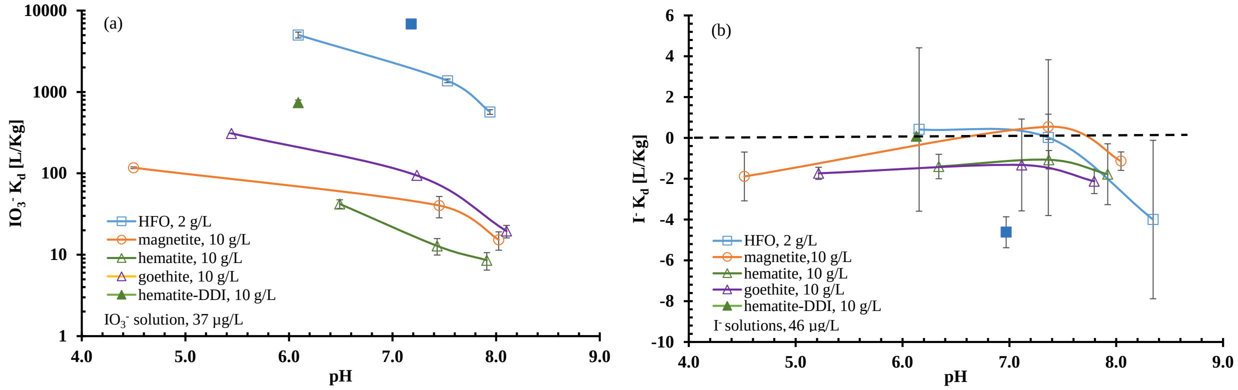

Figure 10. Sorption of a) iodate and b) iodide on HFO, magnetite, hematite, and goethite in the AGW or DDI water systems as a function of pH (pH 4.5 to 8.3) and ionic strength.

3.2.4 Iodine Uptake during HFO Precipitation (co-precipitation)

The iodate and iodide removal efficiencies through co-precipitation with HFO are also presented in terms of a K_d (mL/g), in which the solid mass *m* in Eq. (1) referred to the collected, air-dried solid precipitate weights after all the experimental procedures. Figure 11a shows the determined co-precipitation K_d values for iodate along the four stepwise experimental stages for different times at pH. Figure 11b shows the co-precipitation K_d values for iodide. Like the sorption results, Figure 11 shows much higher co-precipitation K_d values for iodate (~1192 to 1264 mL/g) than for iodide (13 to 36 mL/g). Again, the highest co-precipitation K_d values were found at the lowest pH (pH = 6) conditions for both iodate and iodide. With solution pH increases to pH 6.7 and further to pH 9.2 (10.1 in case of iodide), the co-precipitation K_d deceased dramatically, from 1264 to 73 mL/g and from 36 to 13 mL/g for iodate and iodide, respectively. This trend is the same as the one observed in the adsorption experiments, implying that the co-precipitated IO_3^- or I^- might only attached on the HFO surface through adsorption, whereas any IO_3^- or I^- incorporation into the HFO mineral structure was not likely. However, a K_d value of up to 36 mL/g was observed.

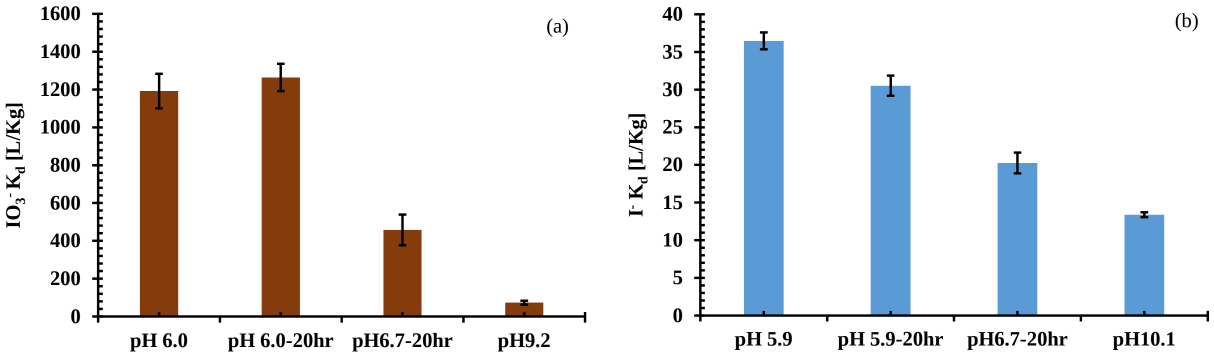

Figure 11. Uptake of a) iodate and b) iodide during HFO precipitations.

The preliminary results to date show that iodate could be effectively removed from the AGW (with the absence of iodine-contaminated sediments) by iron oxides, especially HFO, through either sorption or co-precipitation processes. The high sorption capacity (up to 1300 mL/g for iodate) at near-neutral pH conditions, low cost, simple synthesis methods, and short sorption equilibrium time could made HFO a viable candidate for iodate remediation in the subsurface iodate plumes. For iodide, only limited removal might be reported through the co-precipitation process.

Additional bench-scale testing is needed to quantify sequestration efficiency and longevity of precipitated or immobilized phases containing iodine. Of particular interest is the effect of particle size on iodine adsorption and co-precipitation efficiency. Additionally, information regarding its viability as a field-scale application requires further investigation.

3.3 Enhanced Pump-and-Treat Method

Two mobilization technologies were evaluated for enhanced iodine capture by the pump-and-treat system. Experiments were initiated to investigate mobilization via a strong reductant and via a high pH carbonate solution, and will continue into FY18.

3.3.1 Iodine Mobilization by Na-Dithionite

A carbonate solution (14 mM $NaHCO_3$ at pH 9.3) was developed to slowly exchange uranium out of carbonates by the slow dissolution and precipitation of carbonates (Kohler et al. 2004). This method assumes that uranium co-precipitated in carbonates will re-precipitate carbonates with less uranium substitution. In this study, it was hypothesized that iodine species may also be co-precipitated in carbonates. However, recent extraction data indicates uranium and iodine leaching from sediments differ, suggesting iodine species are not in carbonates. Initial results showed that the addition of the carbonate solution to sediment resulted is a slight increase in aqueous ^{127}I (204 µg/L) at 770 hours (Figure 12b) relative to the 175 to 194 µg/L in the untreated sediment (Figure 12a).

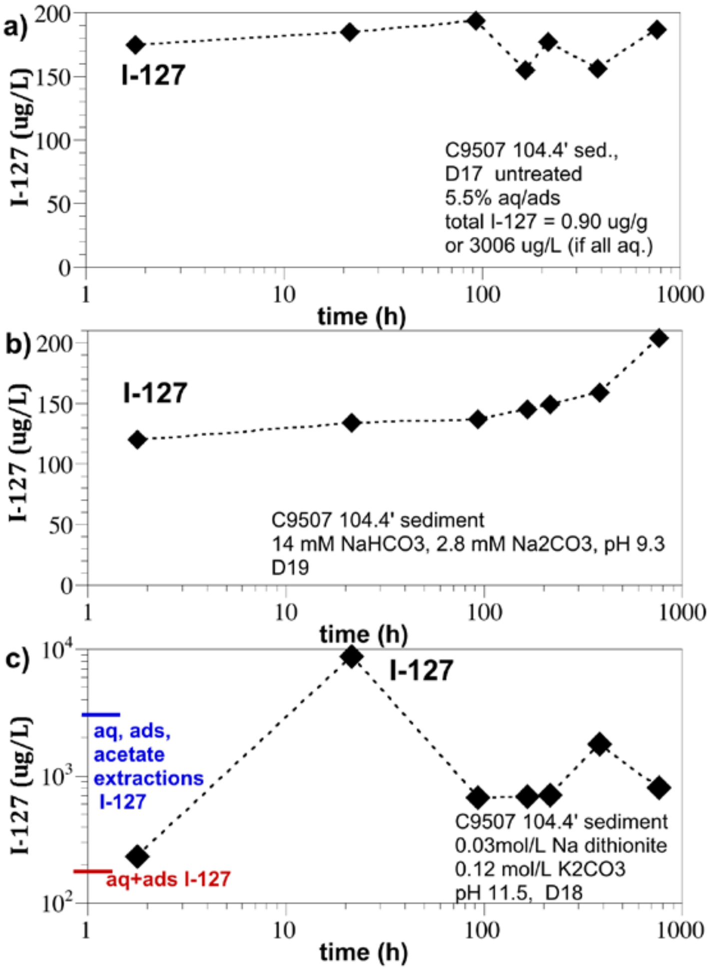

Figure 12. Behavior of iodine-contaminated sediment (C9507, 104.4-105.4') with a) no treatment, b) carbonate solution, and c) sodium dithionite solution. Results are FIO.

3.3.2 Iodine Mobilization by Na-Dithionite

A strong reductant solution (30 mM sodium dithionite, 120 mM K_2CO_3, pH 11.5) was added to the C9507 104.4' sediment for the purpose of reducing aqueous (or carbonate-bound) iodate, as iodide exhibits less sorption than iodate. This reductant also dissolves and reduces ferric oxides to adsorbed ferrous iron and $Fe^{II}CO_3$. It should be noted that if the total ^{127}I extracted from solid phases were in the pore water, the ^{127}I concentration would be 3006 ug/L. Reaction of the dithionite solution with the iodine-contaminated sediment resulted in a significant increase in the aqueous ^{127}I, with inconsistent values ranging between 800 and 8760 µg/L (Figure 12c). While these values could be real (and illustrate a technology to release iodine from sediment by dissolving some surface phases), the results could also be caused by a) dithionite (128 g/mol) interference with ^{127}I measurement on the ICP-MS, or b) iodine contamination in the Na-dithionite or potassium carbonate chemicals. Both of these possibilities are currently being investigated. Extractions of the post-experiment sediment are also under way to evaluate iodine mass balance in the sediment.

4.0 Quality Assurance

The PNNL Quality Assurance (QA) Program is based upon the requirements as defined in DOE Order 414.1D, *Quality Assurance*, and 10 CFR 830, *Energy/Nuclear Safety Management*, Subpart A, Quality Assurance Requirements." PNNL has chosen to implement the following consensus standards in a graded approach:

- ASME NQA-1-2000, *Quality Assurance Requirements for Nuclear Facility Applications*, Part 1, Requirements for Quality Assurance Programs for Nuclear Facilities.
- ASME NQA-1-2000, Part II, Subpart 2.7, Quality Assurance Requirements for Computer Software for Nuclear Facility Applications, including problem reporting and corrective action.
- ASME NQA-1-2000, Part IV, Subpart 4.2, Guidance on Graded Application of Quality Assurance (QA) for Nuclear-Related Research and Development.

The procedures necessary to implement the requirements are documented through PNNL's "How Do I…? (HDI), a system for managing the delivery of laboratory-level policies, requirements, and procedures.

The *DVZ-AFRI Quality Assurance Plan* (QA-DVZ-AFRI-001) was applied as the applicable QA document for this work under the NQA-1 QA program. This QA plan conforms to the QA requirements of DOE Order 414.1D and 10 CFR 830, Subpart A. This effort is subject to the *Price Anderson Amendments Act*.

The implementation of the Deep Vadose Zone – Applied Field Research Initiative QA program is graded in accordance with NQA-1-2000, Part IV, Subpart 4.2, Guidance on Graded Application of Quality Assurance (QA) for Nuclear-Related Research and Development.

The technology level defined for this effort is Basic Research, which consists of research tasks that are conducted to acquire and disseminate new scientific knowledge. During Basic Research, maximum flexibility is desired in order to allow the researcher the necessary latitude to conduct the research. Therefore, any graphs or data presented in this document are "For Information Only," no evaluation was performed as to the accuracy of presented data. As this is an Interim Status report and experiments are still ongoing, required document reviews have not occurred yet.

This work used PNNL's Environmental Sciences Laboratory (ESL) for chemical analyses. The ESL operates under a dedicated QA plan that complies with the *Hanford Analytical Services Quality Assurance Requirements Document* (HASQARD; DOE 2007), Rev. 3. ESL implements HASQARD through *Conducting Analytical Work in Support of Regulatory Programs* (CAWSRP). Data quality objectives established in CAWSRP were generated in accordance with HASQARD requirements. Chemical analyses of testing samples and materials were conducted under the ESL QA Plan.

5.0 Summary and Recommendations

Isotopes of iodine were generated during plutonium production from nine production reactors at the U.S. Department of Energy Hanford Site. Releases of the long half-life ^{129}I to the subsurface have resulted in several large, though dilute, plumes in the groundwater, including the plume in the 200-UP-1 OU and within the vadose zone beneath waste disposal or leak locations. Because ^{129}I is an uncommon contaminant, relevant remediation experience and scientific literature are limited. This document summarizes interim results of laboratory tests to evaluate promising iodine remediation technologies and provides fundamental information needed to determine whether these technologies could potentially be applied for the 200-UP-1 OU plume. Interim evaluation results are provided for four candidate technologies, which include two in situ sequestration methods (apatite, and iron oxides) and two enhanced pump-and-treat approaches. This work provides valuable information required to evaluate remedial technologies for iodine and recommend that additional evaluation efforts continue. This evaluation of potential remediation technology supports the efforts outlined in the *UP-1 Evaluation Plan for Iodine* (DOE 2015, Draft A).

6.0 References

10 CFR 830, *Energy/Nuclear Safety Management*. Code of Federal Regulations, as amended.

ASME NQA-1-2000, *Quality Assurance Requirements for Nuclear Facility Applications*. American Society of Mechanical Engineers, New York, NY.

Campayo L, A Grandjean, A Coulon, R Delorme, D Vantelon, and D Laurencin. 2011. "Incorporation of iodates into hydroxyapatite: a new approach for the confinement of radioactive iodine." *J. Mater Chem.* 2011, 21, 17609-17611.

Chung CW, J Chun, G Wang, and W Um. 2014. "Effects of iron oxides on the rheological properties of cementitious slurry." *Colloids and surfaces A: Physicochemical and Engineering Aspects* 453:94-100.

Couture RA and MG Seitz. 1983. "Sorption of anions of iodine by iron oxides and kaolinite." *Nuclear and Chemical Waste Management* 4:301-306.

Dai JL, M Zhang, and YG Zhu. 2004. "Adsorption and desorption of iodine by various Chinese soils – I. Iodate." *Environment International* 30:525-530.

Dai JL, M Zhang, QH Hu, YZ Huang, RQ Wang, and YG Zhu. 2009. "Adsorption and desorption of iodine by various Chinese soils: II. Iodide and iodate." *Geoderma* 153:130-135.

DOE. 2015. *UP-1 Evaluation Plan for Iodine*. DOE/RL-2015-69, Draft A, U.S. Department of Energy, Richland Operations Office, Richland, WA.

DOE-RL. 2007. *Hanford Analytical Services Quality Requirements Document*. DOE/RL-96-68, Rev. 3, U.S. Department of Energy, Richland Operations Office, Richland, WA.

Emerson HP, C Xu, YF Ho, S Zhang, KA Schwehr, M Lilley, DI Kaplan, PH Santschi, and BA Powell. 2014. "Geochemical controls of iodine uptake and transport in Savannah River site subsurface sediments." *Applied Geochemistry* 45:105-113.

Fuhrmann M, S Bajt, and M Schoonen. 1998 "Sorption of iodine on minerals investigated by x-ray adsorption near edge structure (XANES) and 125-I tracer sorption experiments." *Applied Geochem*. 13:127-141.

Kohler M, DP Curtis, DE Meece, and JA Davis. 2004. "Methods for Estimating Adsorbed Uranium (VI) and Distribution Coefficients of Contaminated Sediments." *Environmental Science and Technology* 38:240-247.

Li H-P, R Brinkmeyer, WL Jones, S Zhang, C Xu, KA Schwehr, PH Santschi, DI Kaplan, and CM Yeager. 2011. "Iodide Accumulation by Aerobic Bacteria Isolated from Subsurface Sediments of a 129I-Contaminated Aquifer at the Savannah River Site, South Carolina." *Applied and Environmental Microbiology* 77(6):2153-2160.

Muramatsu Y, S Uchida, and Y Ohmoto. 1990a. "Determination of I-129 and I-127 in soil and tracer experiments on the adsorption of iodine on soil." *Journal of Radioanalytical and Nuclear Chemistry* 138:377-384.

Muramatsu Y, S Uchida, P Sriyotha, and K Sriyotha. 1990b. “Some considerations on the sorption and desorption phenomena of iodide and iodate on soil.” *Water, Air, and Soil Pollution* 49;125-138.

Nagata T and F Fukushi. 2010. “Prediction of iodate adsorption and surface speciation on oxides by surface complexation modeling.” *Geochimica Et Cosmochimica Acta* 74:6000-6013.

Nagata T, K Fukushi, and Y Takahashi. 2009. “Prediction of iodide adsorption on oxides by surface complexation modeling with spectroscopic confirmation.” *Journal of Colloid and Interface Science* 332:309-316.

Schwertmann U and RM Cornell. 1991. *Iron Oxides in the Laboratory: Preparation and Characterization*. VCH Publishers, Inc., New York.

Soderlund M, M Lusa, J Lehto, M Hakanen, K Vaaramaa, and A Lahdenpera. 2011. *Sorption of iodine, chlorine, technetium, and cesium in soil*. Posiva OY Working Report 2011-04, Eurajoki, Finland.

Strickland C, C Johnson, B Lee, N Qafoku, J Szecsody, M Truex, and V Vermeul. 2016. *Identification of promising remediation technologies for iodine in the UP-1 Operable Unit*. PNNL-26934, Pacific Northwest National Laboratory, Richland, WA.

Ticknor KV and YH Cho. 1990. “Interaction of iodide and iodate with granitic fracture-filling minerals.” *Journal of Radioanalytical and Nuclear Chemistry-Articles* 140:75-90.

Truex M, J Szecsody, N Qafoku, C Strickland, J Moran, B Lee, M Snyder, A Lawter, C Resch, B Gartman, L Zhong, M Nims, D Saunders, B Williams, J Horner, I Leavy, S Baum, B Christiansen, R Clayton, E McElroy, D Appriou, K Tyrell, and M Striluk. 2017. *Contaminant Attenuation and Transport Characterization of 200-DV-1 Operable Unit Sediment Samples*. PNNL-26208,Pacific Northwest National Laboratories, Richland, WA.

Truex MJ, BD Lee, CD Johnson, NP Qafoku, JE Szecsody, JE Kyle, M Tfaily, MMV Snyder, AR Lawter, M Oostrom, G Tartakovsky, II Leavy, EM McElroy, D Appriou, R Sahajpal, MM Carroll, GV Last, MH Lee, and DI Kaplan. 2016. *Conceptual Model of Iodine Behavior in the Subsurface at the Hanford Site*. PNNL-24709, Rev. 1, Pacific Northwest National Laboratory, Richland, WA.

Whitehead DC. 1974. “The sorption of iodide by soil components.” *Journal of the Science of Food and Agriculture* 25:73-79.

Xu C, D Kaplan, S Zhang, M Athon, Y Ho, H Li, C Yeager, K Schwehr, R Grandbois, D Wellman, and P Santschi. 2015. “Radioiodine sorption/desorption and speciation transformation by subsurface sediments from the Hanford Site.” *J. Env. Radioactivity* 139:43-55.

Yu ZS, JA Warner, RA Dahlgren, and WH Casey. 1996. “Reactivity of iodide in volcanic soils and noncrystalline soil constituents.” *Geochimica Et Cosmochimica Acta* 60:4945-4956.

Zachara J, C Brown, J Christensen, JA Davis, E Dresel, C Liu, S Kelly, J McKinley, J Serne, and W Um. 2007a. *A Site-wide Perspective on Uranium Geochemistry at the Hanford Site*. PNNL-17031, Pacific Northwest National Laboratory, Richland, WA.

Pacific Northwest
NATIONAL LABORATORY

U.S. DEPARTMENT OF
ENERGY

Proudly Operated by **Battelle** *Since 1965*

902 Battelle Boulevard
P.O. Box 999
Richland, WA 99352
1-888-375-PNNL (7665)

www.pnnl.gov